2013-01-01

3D Printed Impedance Elements By Micro-Dispensing

Ubaldo Robles Dominguez
University of Texas at El Paso, urobles@miners.utep.edu

3D PRINTED IMPEDANCE ELEMENTS BY MICRO-DISPENSING

UBALDO ROBLES DOMINGUEZ

The Department of Electrical and Computer Engineering

APPROVED:

Raymond C. Rumpf, PhD.,Chair

Eric MacDonald, PhD.

Peter Kim, PhD.

Benjamin C. Flores, Ph.D.
Dean of the Graduate School

DEDICATION

To my family, especially to my wife, who have helped me focus on today's efforts towards a better career.

3D PRINTED IMPEDANCE ELEMENTS BY MICRO-DISPENSING

By

UBALDO ROBLES DOMINGUEZ BS in EE

THESIS

Presented to the Faculty of the Graduate School of

The University of Texas at El Paso

in Partial fulfillment

of the Requirements

for the Degree of

MASTER OF SCIENCE

Department of Electrical and Computer Engineering

THE UNIVERSITY OF TEXAS AT EL PASO

May 2013

ACKNOWLEDGEMENTS

This work was funded in part by a grant from:
Lockheed Martin Missiles and Fire Control, Orlando, Florida.

EM Lab Team:

Paul Deffenbaugh
Harvey Tsang
Dr. Raymond Rumpf

W.M. Keck Center for 3D Innovation

University of Texas at El Paso

ABSTRACT

Micro-dispensing allows electric circuits to be "3D printed," which can be used to give 3D printed systems electronic and electromagnetic functionality. The focus of this thesis is using micro-dispensing to fabricate capacitors and inductors. 3D printed impedance elements are capable of being more easily embedded, can be used to create structural electronics, and will have extensive applications in antennas, metamaterials, frequency selective surfaces, and more. This is the first known effort to print and measure impedance elements by micro-dispensing which holds great potential for manufacturing multi-material devices.

TABLE OF CONTENTS

LIST OF TABLES

LIST OF FIGURES

CHAPTER 1
PURPOSE

There is tremendous demand to simultaneously miniaturize and add functionality to electromagnetic systems. Needs span from miniaturizing metamaterials to modifying the performance of antennas. Many techniques for doing this are based on introducing impedance elements (i.e. resistance, inductance and capacitance) into the structure. This approach, however, can lead to prohibitively complex designs are expensive to build and tedious to populate. Recently, additive manufacturing (AM) has matured to the point where it can produce the end product directly instead of just rapid prototypes. AM can form very complex three-dimensional geometries and seems ideally suited for manufacturing complex structures with integrated circuits including printed impedance elements. There exists, however, some challenges and many questions about state-of-the-art and what performance and tolerances are achievable.

The primary goal of this effort is to determine what ranges of impedance values are possible, determine performance criteria, and identify any major weaknesses of printed impedance elements. The secondary goal is to develop printed impedance elements with maximum impedance in minimum space. While a number of AM technologies are available at UTEP, this project focused on the nScrypt micro-dispensing system.

1.1 Research Summary

In this effort, inductors were printed with overall dimensions around 2.2 mm with inductance around 150 nH. While values of 200 nH are possible with simple structures. Higher values can be reached by incorporating magnetic materials or using more sophisticated elements.

Capacitors were printed with overall dimensions around 5.0 mm with capacitance in the 10 to 12pF range. Although 20pF values are possible with the simple structures the use of high dielectric materials and the use of multilayers can improve the performance of the device.

Overall, the weakness of this project resides on the thickness of the material later that will limit the maximum value of the capacitance. Thin film capacitors have layers in the order of

10nm while printed lines are in the order of 30μm. Second, controlling the flatness of the surface comes to be a challenge critical to produce consistency between prints.

CHAPTER 2
PROCEDURES

3D printing holds great promise to revolutionize manufacturing. Over the last ten years, 3D printing has evolved from a rapid prototyping tool to a true manufacturing technology capable of producing functional products. However, the majority of products today contain electronic and electromagnetic functionality. In order to manufacture these products by 3D printing, it will be necessary to print the electronic and electromagnetic components.

There exists a wide variety of 3D printing technologies [1], but it is not yet certain which will emerge as the dominant approach. At present, two seem most capable for printing electrical components. The Dimatix tool by Fujifilm is an inkject process that deposits pico-liter drops onto a flat substrate. It is capable of printing very high resolution patterns, but is limited to printing in just two dimensions [2]. It will be very difficult to extend this technology to true 3D printing. At present, micro-dispensing seems most promising for 3D structures with embedded electrical components. Micro-dispensing is a technique that deposits materials in liquid or paste form in volumes down to less than a microliter. It is rapidly evolving into a multi-material 3D printing technique that will enable truly three-dimensional structures to be manufactured [3]. It can also be hybridized with other 3D printing techniques, and has already been demonstrated for printing antennas and electrical interconnects [4], [5]. In this work, we used an nScrypt-3Dn-600 for printing. The tool is capable of scanning irregular surfaces and dispensing up to four different materials onto that surface. It is equipped with a vacuum chuck to hold substrates securely in place and to keep flexible substrates flat. The tool is also equipped with sensors and cameras for alignments, scanning the shape of a surface, and recording the printing process.

This project presents our preliminary work printing inductors and capacitors by micro-dispensing. These components are the fundamental building blocks of electronic circuits. Impedance elements are used in power conditioning, analog and RF filters, driving sensors and displays, loading antennas, and much more.

2.1 DESIGN METHODOLOGIES

2.1.1 Electromagnetic Design

This project began by studying a number of simulation method including closed form equations, online calculators, simple finite-difference solutions, and commercial simulation packages. The team started with online calculators to get a first-order approximation of device dimensions and impedance values. By the end of the project, commercial packages like Ansoft Designer and HFSS were used because they could incorporate electromagnetic properties of materials, field fringing, and more. Ansoft Designer® proved to be the most effective approach for this project. It was easy to use and could simulate impedance elements of arbitrary shape. Inductors with hexagonal, octagonal, circular, and square spiral coils were considered, but circular because the preferred approach. Figure 2.1shows the simulated inductance of a four-turn spiral inductor designed to provide a 36 nH inductance. The overall size of this device is just over 2 mm. The circular spiral coil showed improved impedance values over the rest as well as smaller features [6].

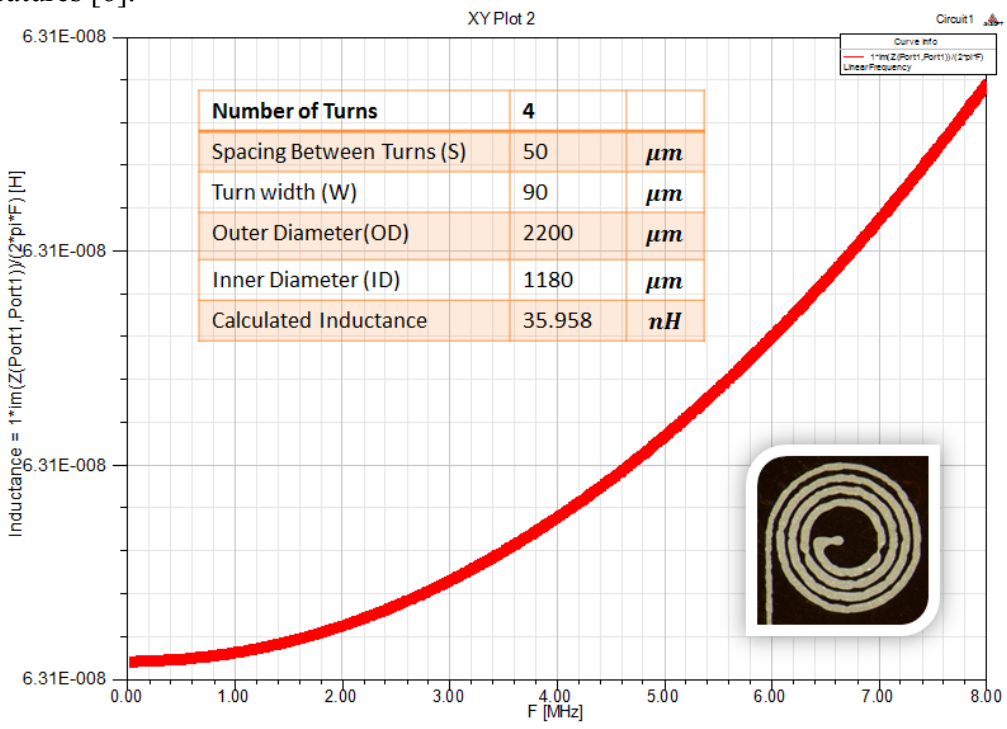

Figure 2.1: Simulation of 36 nH printed inductor.

The interdigitated capacitor design was chosen due to its common use in microstrips. Capacitance control, high Q values, and low parasitic capacitance are desired features that were taken into account in the selecting a capacitor design [7]. Figure 2.2 shows the simulated capacitance of a 4 pF interdigitated capacitor. Through simulation, it was found that small spacing between the lines will be critical for achieving higher capacitance values.

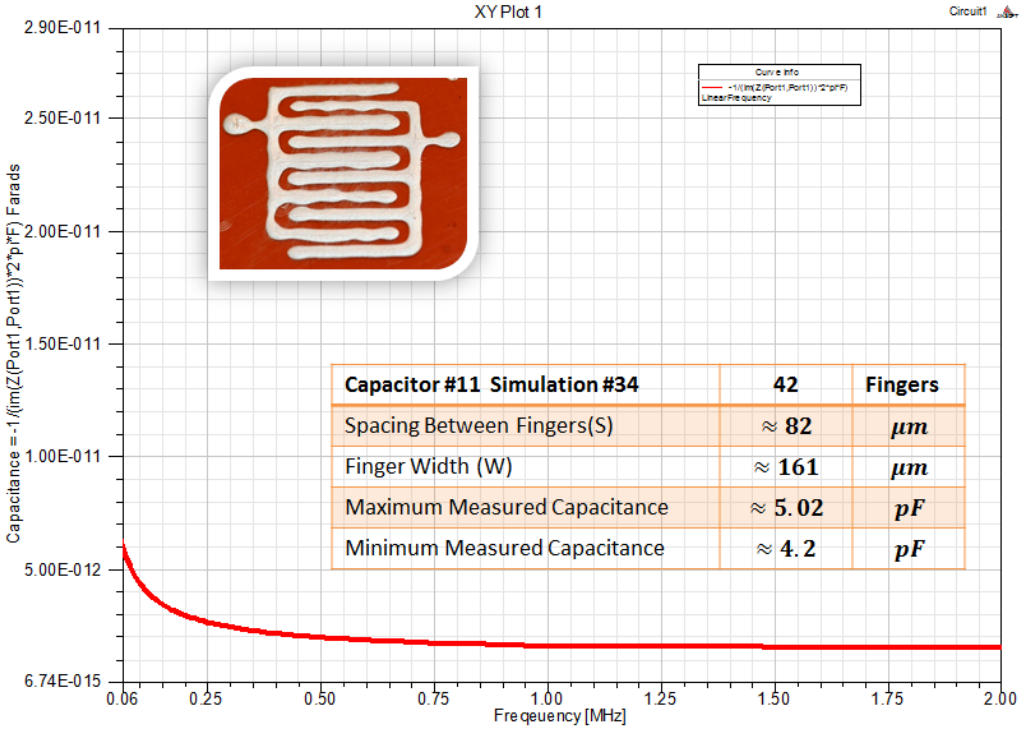

Figure 2.2: Simulation of a 4 pF printed capacitor

2.2.2 LAYOUT

Layout of the capacitors was easy and was successfully performed and simulated in Ansoft Designer, SolidWorks, as well as nScypt's custom MtGen3 CAD software. For inductors, none of these CAD packages had a tool for generating flat spiral geometries. In steady, custom codes were written in MATLAB to generate these geometries and save them to a DXF file. The file could then be read into any of the CAD packages to complete the designs. The MATLAB code is provided in Appendix A at the end of this document. Initially, designs were laid out in HFSS because that was the tool the team was using to design devices. When this

tool was abandoned as the tool to start device design with, SolidWorks was used and could add useful features like probe signal pads, green dielectrics, and substrates.

2.3 MANUFACTURING METHODOLOGIES

Two tools were considered in this project. These were the nScrypt micro-dispensing system and the Dimatix piezoelectric inkjet. Of these, the nScrypt tool was favored because of its versatility and potential for true 3D printing.

2.3.1 Dimatix DMP-2800 Printer

The Dimatix printer deposits fluidic materials onto substrates up to 8.5"×11" using a disposable inkjet cartridge. This printer can handle substrates up to 25 mm thick with an adjustable z height. Each cartridge has a capacity of 1.5 ml and can be changed to print different fluids. They each have 16 nozzles linearly spaced 254 mm apart with typical drop sizes of 1 to 10 picoliters. The machine can maintain a positional accuracy around 5 μm. It uses a temperature controlled vacuum platen to handle the substrates during printing. Substrate materials include plastic, glass, ceramics, silicon, and flexible substrates such as membranes, gels, thin films, and paper. The Dimatix printer and a cartridge are provided in Figure 2.3.

Figure 2.3: (Left) DMP-2800 printer. (Right) "Inkject" cartridge.

A key goal of the project was to manufacturing measurable devices before scaling down the size or adopting more sophisticated designs. The Dimatix is able to deposit picoliter droplets that can achieve lines widths of 10 μm and with 5 μm spacing. However, it is difficult to control

the fluidity of the materials composed with silver nanoparticles. In addition, the uncertainty of the inks is another variable to add to our initial designs [2]. As a result, this approach was abandoned and work focused on the nScrypt micro-dispensing system.

2.3.2 Printing on the nScrypt 3Dn-600-HPx

The nScypt 3Dn-600-HPx can print over a 600 mm × 600 mm area and achieve feature sizes below 50 µm using SmartPump™ technology. It is equipped with four dispensing heads for printing multiple materials, UV curing for printed resins, a downward-facing fiducial-find camera, a pick-and-place robot with auto-tool change, and a laser height scanner which enables conformal printing on curved surfaces.

Figure 2.4: Micro-dispensing of a preliminary interdigitated capacitor

The first step for printing is to generate a DXF file containing the CAD drawing of the desired print. Using nScrypt's PCAD software, this DXF file is converted to a print path script file which contains the XYZ move commands as well as pump on/off commands. This software converts all solid surfaces into a series of lines with some given line width [4]. This process is illustrated in Figure 2.5. The resulting script file is loaded into Machine Tools Generation 3 (MTGen3), the machine software. The script is added to a project file as a print job and combined with other jobs for fiducial-find and conformal printing.

To prepare the pump for printing, the material of choice (DuPont CB028 silver flake polymer ink) is loaded into a syringe (3 cc) which is then screwed into the pump and an air pressure supply line is connected to the back end of the syringe. This pressure will be set as a process parameter and the flow of the ink is controlled by nScrypt's patented pumping system. A conical ceramic pen tip (125 μm I.D. x 175 μm outer diameter) is attached to the end of the pump. The inner diameter of the tip is determined based on the maximum particle size of the material. CB028 is known to have a particle size of about 10 μm. The inner diameter of the pen tip must be 10 to 20 times larger than the maximum particle size for reliable and clog-free printing. The outer diameter of the tip is the primary factor in producing a particular line width. Generally, line widths are adjusted through a combination of tip outer diameter (175 μm), print speed (~10 mm/s), and height above the surface (50 μm). The minimum line width is typically approximately equal to the outer diameter of the tip. Height above the surface is also critically important because if the tip is not close enough, the polymer ink (with a consistency of nail polish) will not adhere to the surface during printing but rather form globs attached to the sides of the tip. This is why conformal mapping using the laser displacement sensor is necessary to maintain consistent control of the height above the surface. Once the pump is prepared and the machine has been calibrated the print project is loaded and executed in MTGen3 on the machine [4]. Initially, the process is very operator intensive because all of the system parameters (see list below) must be tuned for the material properties and substrate characteristics. Through an iterative process of parameter adjustment the process is optimized and assuming the given parameters (required line width and material properties) are within acceptable ranges, a successful print will be possible.

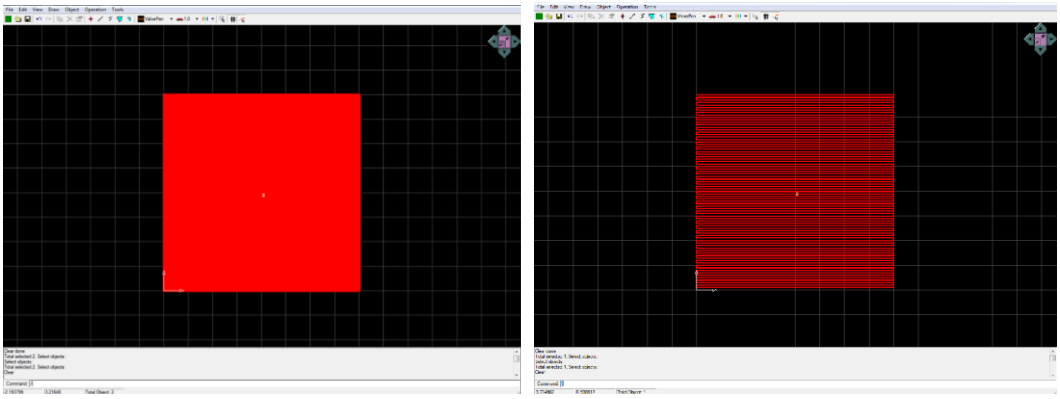

Figure 2.5: (Left) Initial CAD design. (Right) Design converted into line paths using MtGen3.

2.3.3 Inks

Silver-flake polymer ink was used for printing the conductive traces of the impedance elements. These inks consisted of micron-sized silver flakes suspended in a thick film polymer, similar to nail polish. An ideal ink has small particles (to avoid clogging), does not dry in air at room temperature, and cures at relatively low temperature to avoid damaging printed resin substrates, and has excellent conductivity when fully cured.

The initial trials for this project were printed with expired ink (Ercon E1660) which created a number of problems. Over time, the silver particles agglomerate, or clump together, giving the ink inconsistent effective viscosity properties and thus clogging the micro-dispensing head. At best, this makes the process parameters fluctuate during the printing making fabrication difficult to control and be consistent. Old ink also dries too quickly making discontinuous prints difficult because the ink has a tendency to dry on the tip in air between prints. To overcome the clogging problem a larger pen tip which prints very wide lines had to be used in order to form working elements. Subsequent trials with new ink of a preferred type (DuPont CB028) produced excellent structures with fine feature sizes. Figure 2.6 covers the explanation regarding how the expired ink was barely able to produce line widths less than 1 mm. New inks could print features below 0.1 mm.

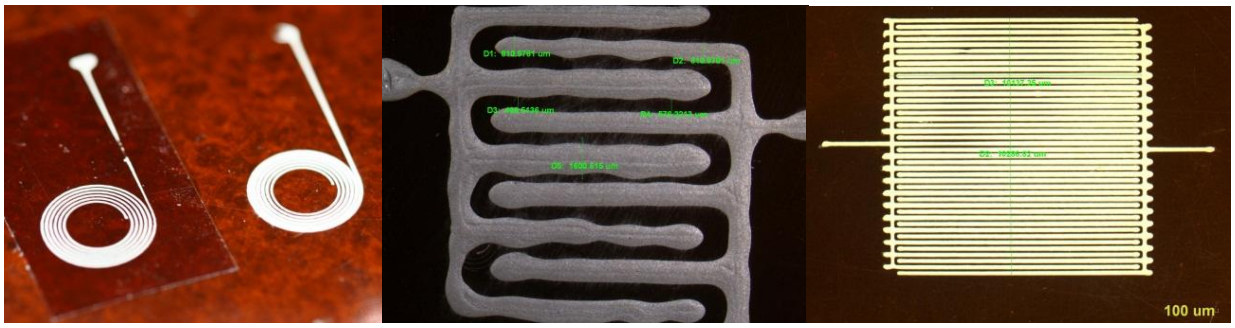

(a) expired ink, (b) expired ink, (c) new ink.

Figure 2.6: Comparison between expired ink and new DuPont CB028

2.3.4 Surface Control

The surface height of a substrate can vary by hundreds of microns. This becomes significant when printing lines with these same feature sizes. When a new ink is loaded into the SmartPump™, it is first necessary to find the correct valve parameters to produce clean lines and line starts. The width of lines is controlled through air pressure, SmartPump™ movement speeds, and gap height from the pen tip to the substrate. Acceleration and deceleration of the SmartPump™ through corners also requires special attention. Speeds that are too fast result in broken lines while speeds that are too slow result in material build up.

The nScrypt machine is outfitted with height scanning sensors and fiducial cameras that make printing on the fluctuating substrates possible, but surface flatness must be controlled much more precisely to obtain repeatable prints with very small feature sizes (less than 50 μm). Accurate printing was possible due to a flat vacuum chuck that ensured flatness to within ±10 μm. In principle, the z-scanning sensor is accurate enough to avoid the need of the vacuum chuck, but scanning such a large area at such a high resolution leads to scan times and files sizes that are not feasible for this effort. The vacuum chuck was the most economical and versatile solution for this effort.

2.4 TEST AND EVALUATE CANDIDATE ELEMENTS

2.4.1 Test Equipment and Setup

Three pieces of test equipment were available for this effort. Each of these is shown in Figure 2.7. The Agilent LCR meter covers 20 Hz to 20 MHz and was the easiest and most straightforward equipment to use for this project. The Agilent impedance analyzer covers 1 MHz up to 3 GHz and is capable of making more precise measurements at the higher frequencies. In future work, all measurements will be taken both the LCR meter and impedance analyzer and compared.

Figure 2.7: Impedance element measurement setup.

One at a time, the impedance elements were mounted into a probe station (model 6000-AO, Micromanipulator, Inc.) to facilitate measurement and to avoid motion during the measurements. Two gold plated probes (model 7B, Micromanipulator, Inc.) were pressed into contact with the measuring ports of the impedance element. The impedance values were measured with an Agilent E4980A Precision LCR Meter. The setup was calibrated before every measurement. We tested our measurement procedure by mounting known chip capacitors and inductors with 1% tolerances onto printed silver ink pads on Kapton. Figure 2.8 shows a photograph of our measurement setup.

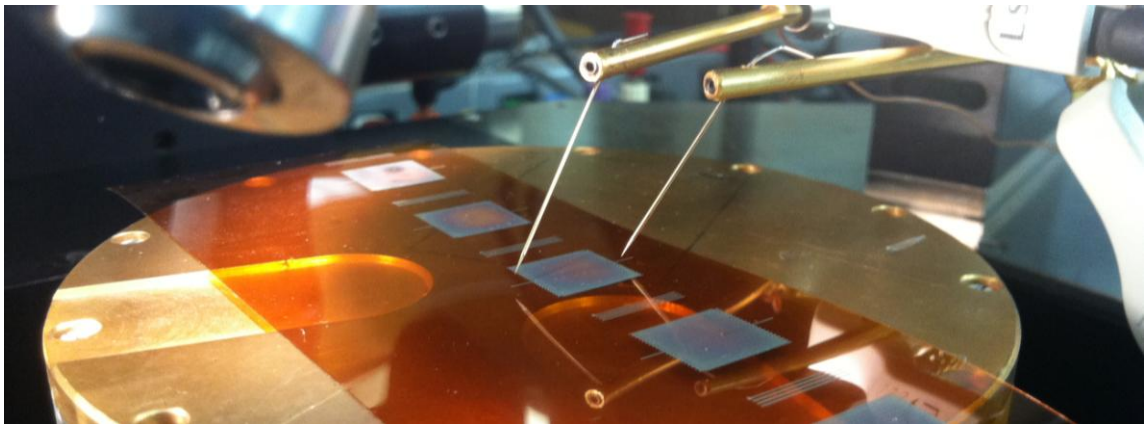

Figure 2.8: Shows a photograph of our measurement setup

2.4.3 Benchmark Measurements

To validate the setup and confirm the accuracy of the measurements, the impedance of off-the-shelf chip elements were measured. Data from a 10 pF chip capacitor with 1% tolerance is shown in Figure 2.9. Measurements obtained in the lab matched the specified value within 2% over the frequency range of 100 kHz to 2 MHz. In fact, the measurements are likely better than this because the 1% tolerance on the chip capacitor is only specified at a single frequency.

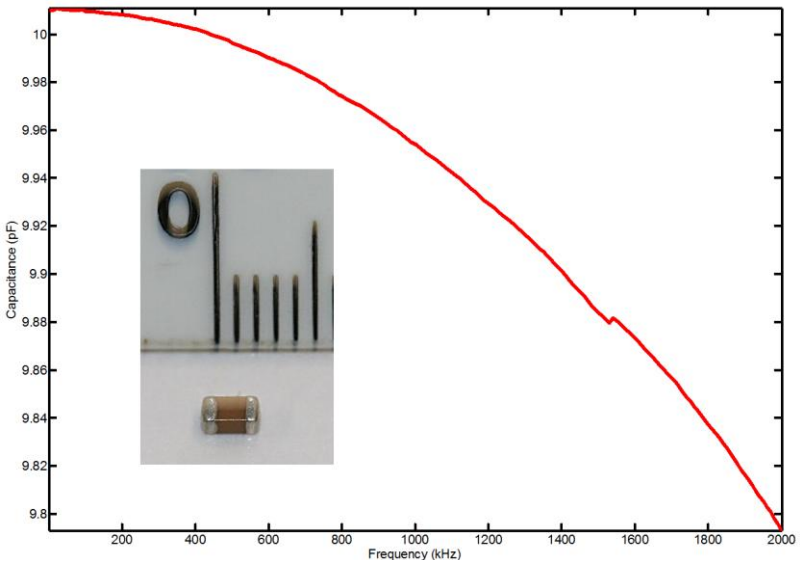

Figure 2.9: Benchmark measurement of a 10 pF chip capacitor

CHAPTER 3
IMPEDANCE ELEMENT DESIGN

Ultimately, the capability is needed to 3D print the basic circuit elements with controllable values and reasonable tolerances. To reduce the variables in this initial work, we focused on printing planar elements without any dielectric or magnetic loading. To better assess and calibrate our work, we proceeded with well-known spiral inductors and interdigitated capacitors. The following sections outline our designs and methodologies.

3.1 CANDIDATE ELEMENTS FOR CAPACITANCE

We also used ANSYS Designer® to design an interdigitated capacitor to be 12 pF [7]. The outer dimension of the capacitor was just over 5.0 mm. In chapter 4 the final results compares the modeled parameters to the measured. Furthermore, the model results versus the measured results from the constructed devices are covered according to the generational attempts.

3.1.1 Design

Planar interdigitated capacitors were chosen for this short two-month effort in order to most effectively assess the device tolerance that could be achieved. Incorporating multiple layers, high dielectric constant materials, and complex geometries will certainly boost capacitance, but would introduce more variables to be controlled. More sophisticated capacitor designs will be explored when the simpler designs can be produced within the required 2% tolerance. The main goal for the past two months was to achieve a $10\,\mathrm{pF/mm^2}$ interdigitated capacitor with 100 μm features.

3.1.2 Capacitor Generations

According to model, the team performed several attempts to print an interdigitated capacitor. Five generations of integrated capacitors were built before the ideal device was printed. The most difficult variables to attain were surface flatness.

A quick experiment was performed where a capacitor was printed onto a Kapton dielectric with a ground plane. This device provided nearly eight times the capacitance as a similar device without the ground plane. This is because the ground plane provided additional surface area and hence increased capacitance. This shows that significant increase in capacitance will be possible with alternate designs.

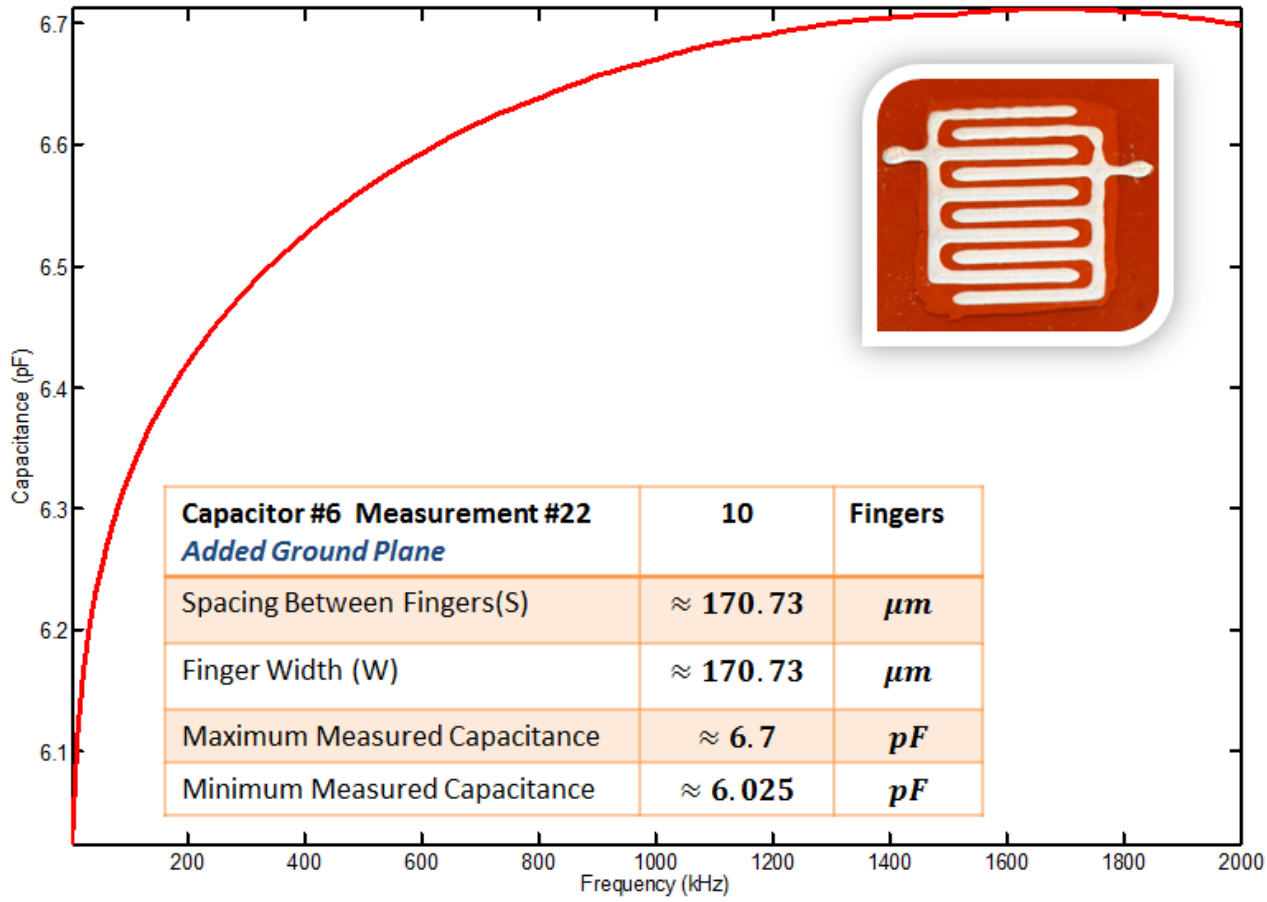

Figure 3.1: Capacitor with ground plane

The measured capacitance from a first-generation printed capacitor is provided in Figure 3.2. This device was designed to provide 5 pF of capacitance. It was measured to be around 1.7 pF. The discrepancy was due to using expired ink and not being able to control the print reliably.

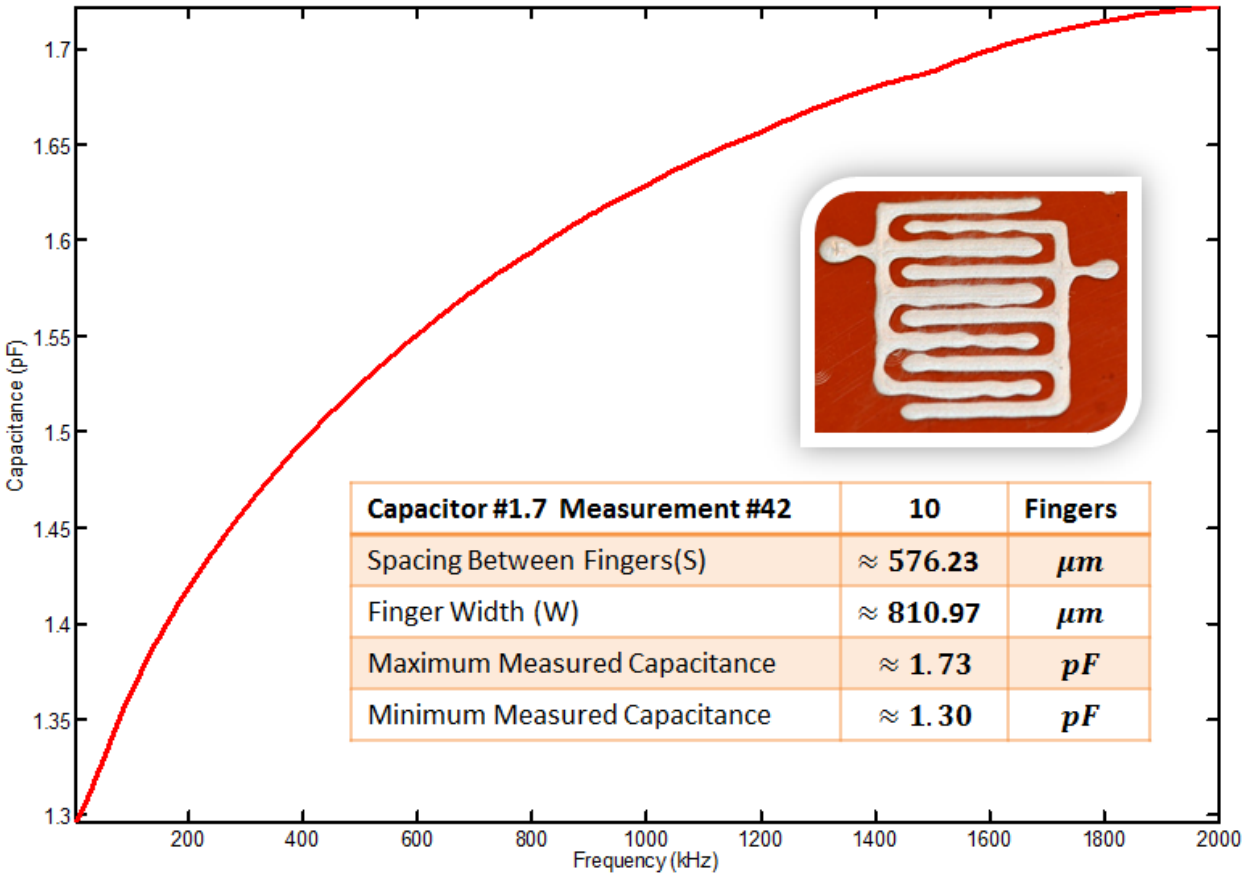

Figure 3.2: Measurement of a first-generation printed capacitor.

The measured capacitances from two different third-generation printed capacitors are provided in Figure 3.3 and Figure 3.4. The capacitor shown in Figure 19 was design to be 20 pF, but was measured at 10.42 pF. The design called for 100 μm lines and 50 μm spaces, but the print gave a device with 180 μm lines and 70 μm spaces. This reduced the capacitance by nearly 50%.

A second third-generation capacitor is shown in Figure 3.4. The fingers on this design were around 10× shorter resulting in a 10× reduction in capacitance.

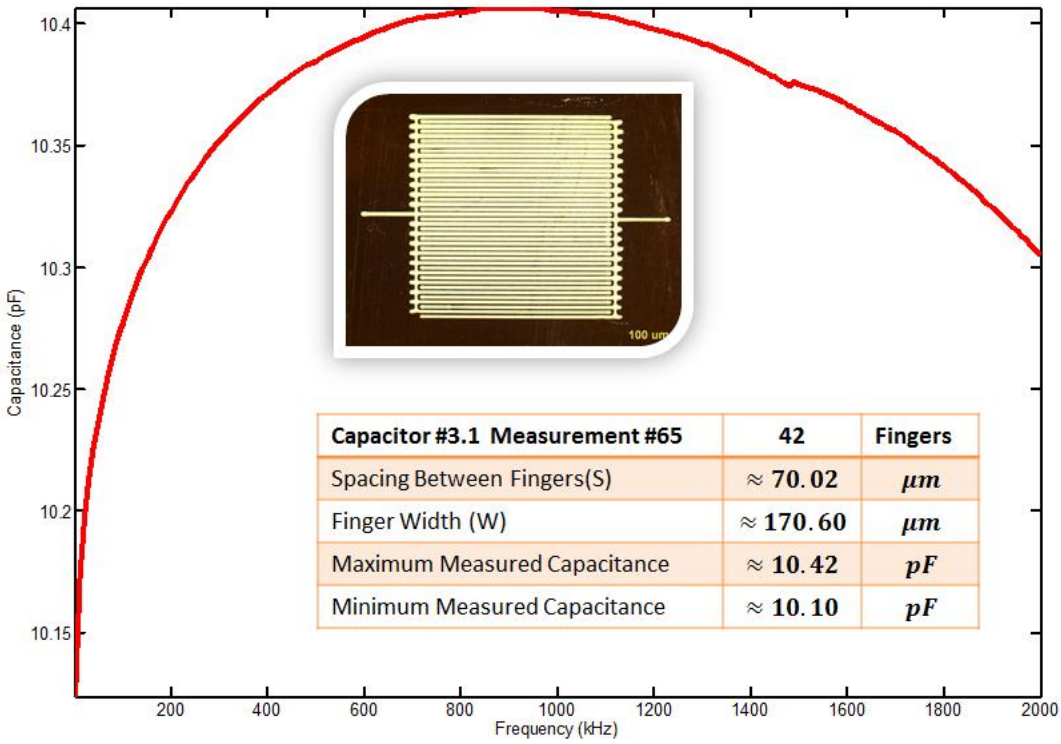

Capacitor #3.1 Measurement #65	42	Fingers
Spacing Between Fingers(S)	≈ 70.02	μm
Finger Width (W)	≈ 170.60	μm
Maximum Measured Capacitance	≈ 10.42	pF
Minimum Measured Capacitance	≈ 10.10	pF

Figure 3.3: Measurement of a third-generation printed capacitor

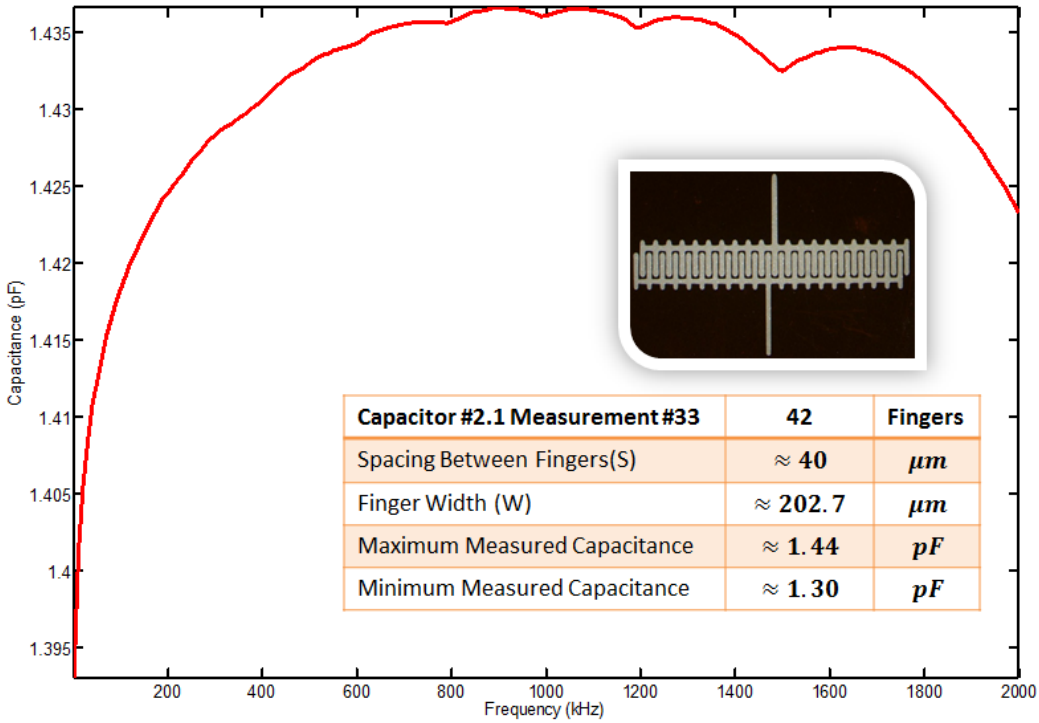

Capacitor #2.1 Measurement #33	42	Fingers
Spacing Between Fingers(S)	≈ 40	μm
Finger Width (W)	≈ 202.7	μm
Maximum Measured Capacitance	≈ 1.44	pF
Minimum Measured Capacitance	≈ 1.30	pF

Figure 3.4: Measurement of a second 3rd-generation capacitor

3.1.4 Importance of Line Spacing

A short study was performed through simulation to explore the important and effect of line spacing on capacitance. Data from this study is provided in Figure 3.5. The total capacitance exponentially increases with decreasing line spacing. The conclusion is that it will be important to have small line space to maximize the capacitance produced from an element. Fortunately, line spacing is more easily reduced than line width in micro-dispensing. Some elements were already produced with 50 μm spacing. With further work, it should be possible to reduce this even further.

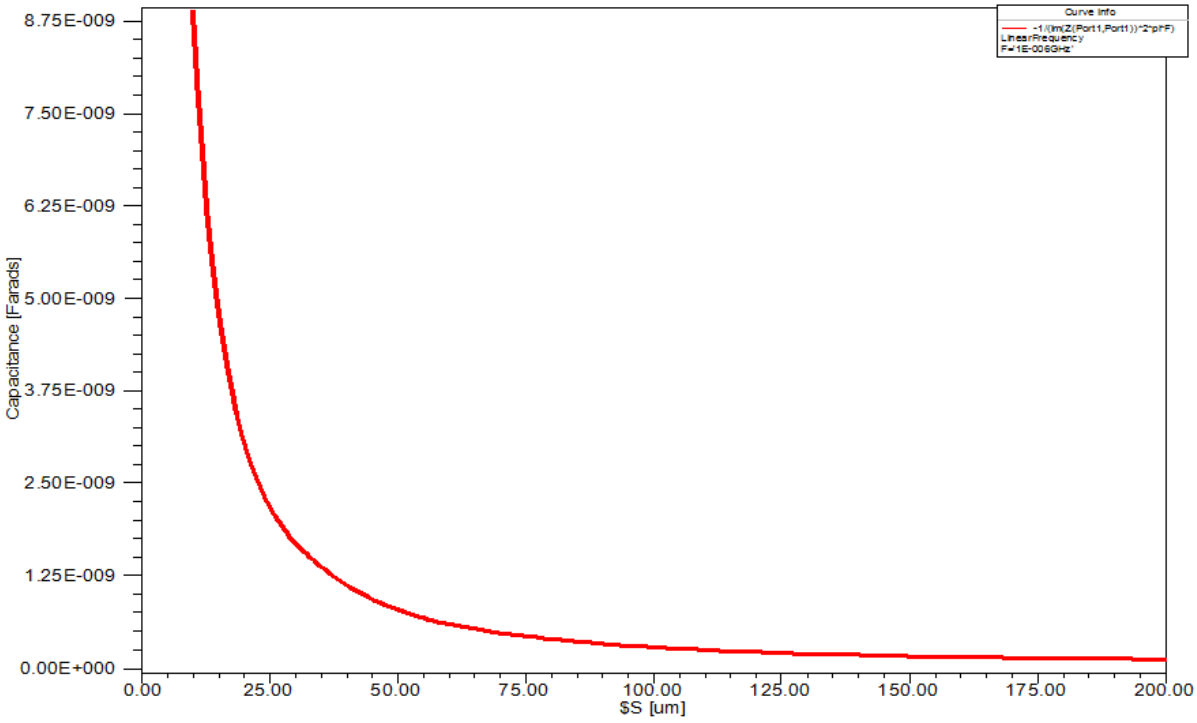

Figure 3.5: Capacitance as a function of line spacing.

3.1.5 Fabrication

The first generation of capacitors was printed onto Kapton using expired ink. Representative images are shown in Figure 3.6. Adhesion to the substrate was excellent. As discussed previously, lines and spaces were limited to features on the order of 1 mm due to the

poor properties of the expired ink. Capacitance values were on the order of 4 pF and overall dimensions of the elements were on the order of centimeters.

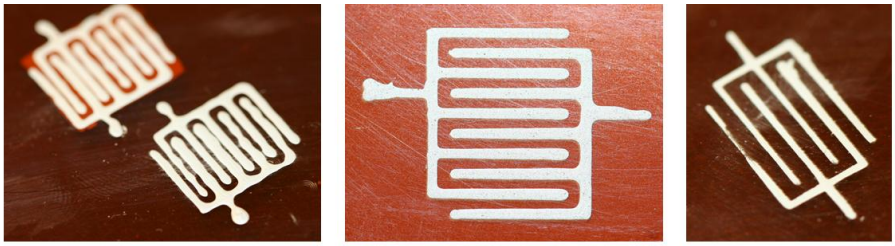

(a) first generation capacitors with expired ink

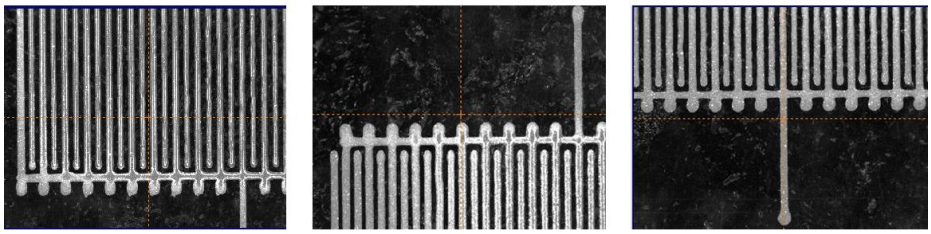

(b) second generation capacitors with new CB028 ink

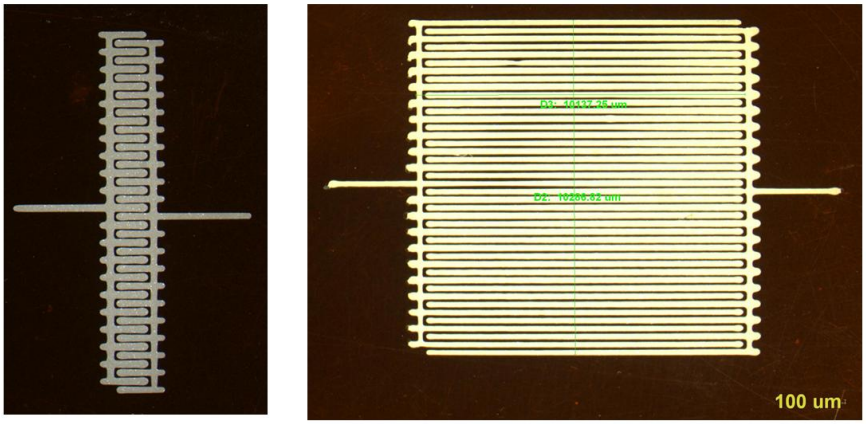

(c) third generation capacitors with new CB028 ink

Figure 3.6: Sequence of capacitor designs achieved during the two-month project

The second generation of capacitors was printed using new ink from DuPont (CB028) onto packing tape. The structures were well formed with dimensions on the order of 100 μm. Initially, adhesion to the tape seemed okay, but after one week the traces peeled off of the substrate making testing of the devices impossible.

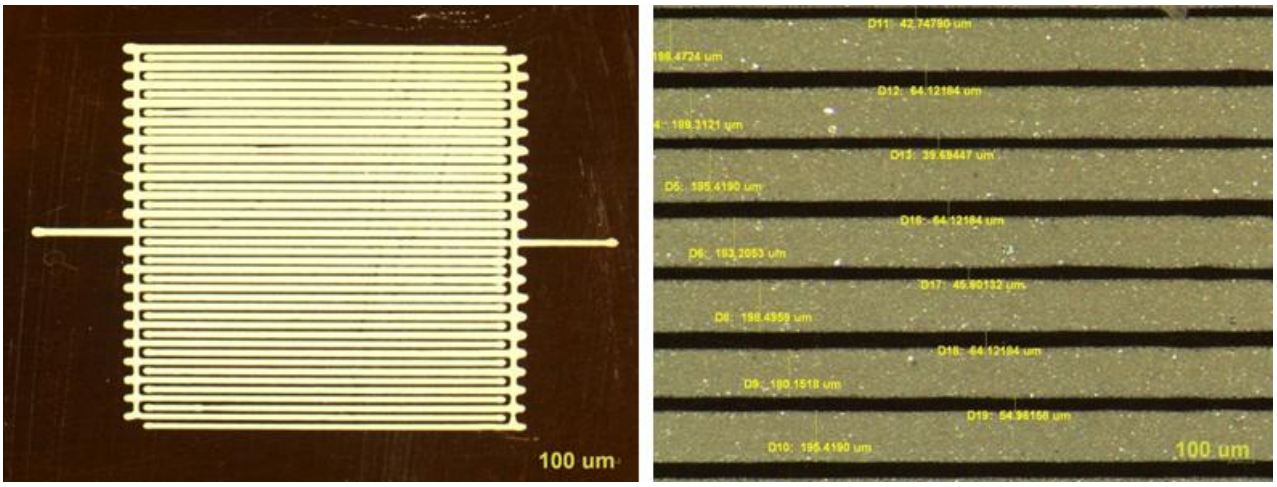

Figure 3.7: Close up of interdigitated capacitor and its line features

3.2: CANDIDATE ELEMENTS FOR INDUCTANCE

3.2.1 Design

Planar spiral inductors were chosen for this short two-month effort in order to most effectively assess the device tolerance that could be achieved. Incorporating more spirals, high permeability materials, and complex geometries will boost inductance, but would introduce more variables to be controlled. Further, the required inductance values are achievable using these simple structures. The inductor design considered spirals shaped like hexagons, octagons, circles, and squares. Of these, the circular spiral inductor was the selected. They provided high inductance from a continuous line that can be printed more consistently than a pattern with discrete bends. These were designed for 36 nH and simulations showed this was easily achieved in the desired form factor.

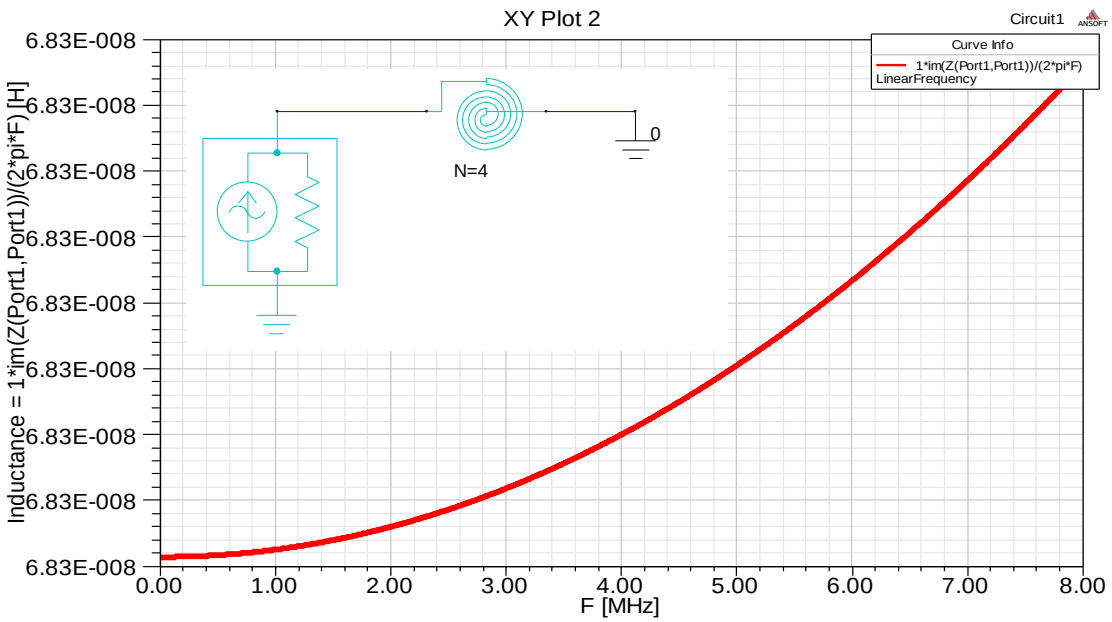

Figure 3.8: Ansoft Designer planar spiral inductor

3.2.2 Fabrication

The first generation of inductors was printed onto Kapton using expired ink. Representative images are shown in Figure 3.9. Adhesion to the substrate was excellent. As discussed previously, lines and spaces were limited to features on the order of 1 mm due to the poor properties of the expired ink. Simulated inductance values were on the order of 36 nH and overall dimensions of the elements were on the order of centimeters.

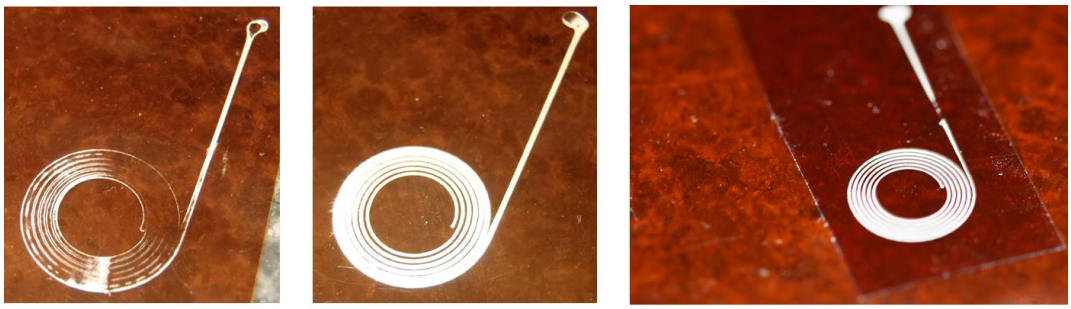

(a) first generation inductors with expired ink on kapton

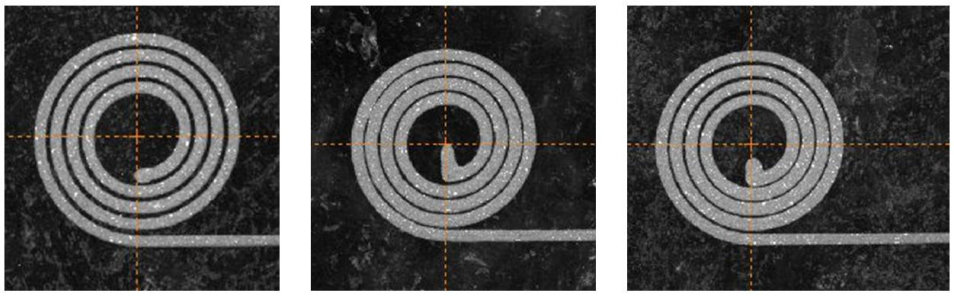

(b) second generation inductors with new CB028 ink on packing tape

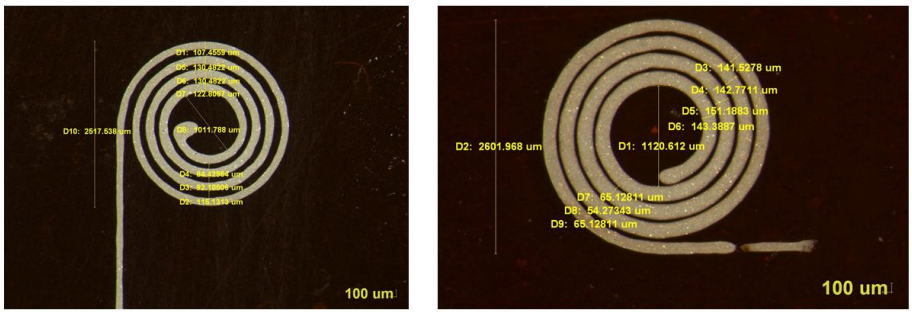

(c) third generation inductors with new CB028 ink on kapton

Figure 3.9: Sequence of inductor designs achieved during the two-month project

The second generation of inductors was printed using new ink from DuPont (CB028) onto packing tape. The structures were well formed with dimensions on the order of 100 μm. Like the second generation of capacitors, these peeled from the substrate after just one week.

The third generation of inductors was printed with the same material on Kapton to prevent adhesion issues. The dimensions were still on the order of 100 μm.

To assess dimensional tolerances, a final batch of four-turn inductors was printed using the new CB028 ink on Kapton. Some of these are shown in Figure 3.10. The process

parameters were kept constant so the variations were due solely to fluctuations in the height of the substrate. The substrate height varied by no more than 15 μm confirming the importance of printing on a flat substrate to obtain consistent results.

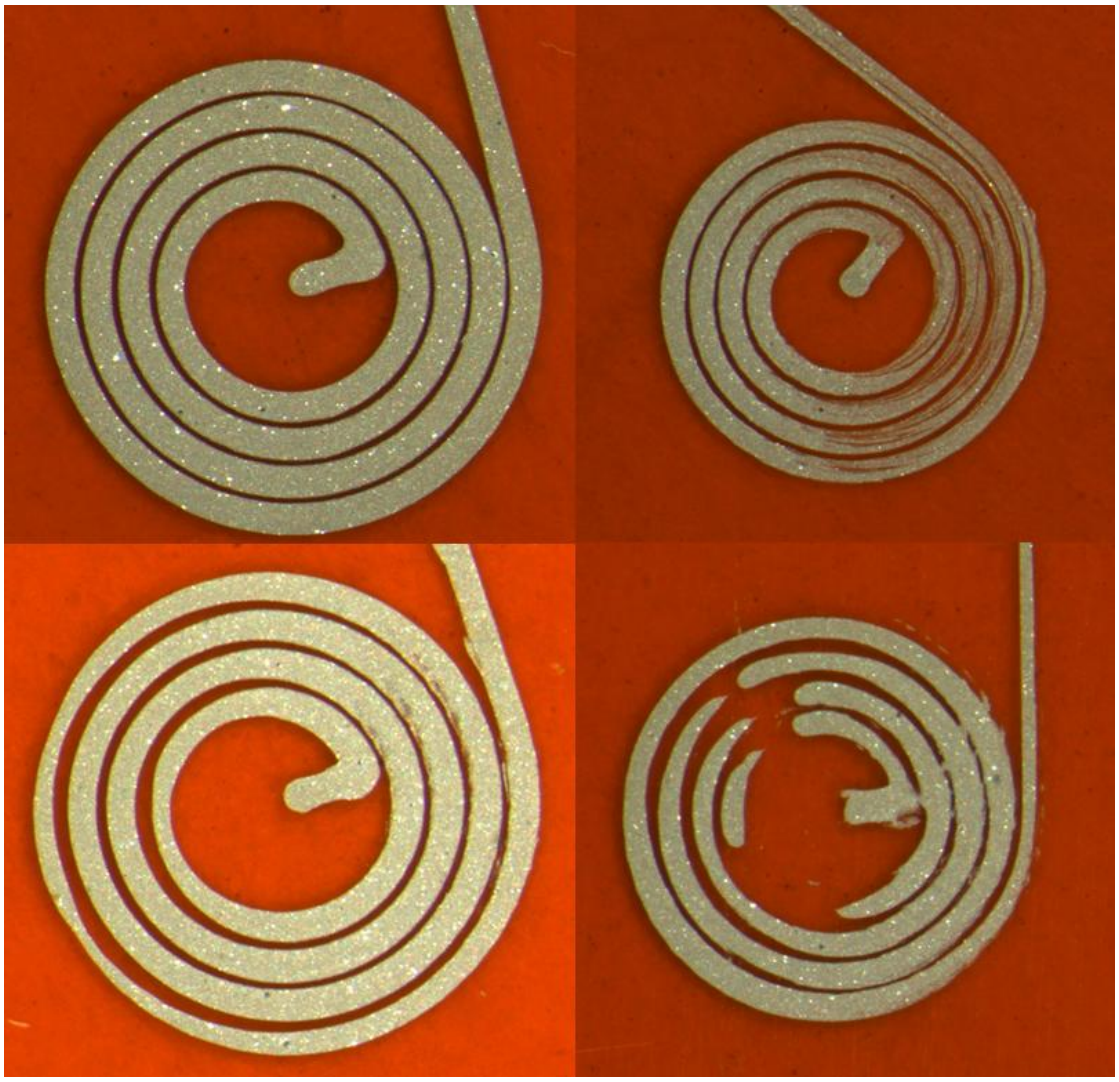

Figure 3.10: Four spiral inductors from a batch of 14 using consistent print parameters

CHAPTER 4
RESULTS

Ultimately, the capability is needed to 3D print the basic circuit elements with controllable values and reasonable tolerances. To reduce the variables in this initial work, we focused on printing planar elements without any dielectric or magnetic loading. To better assess and calibrate our work, we proceeded with well-known spiral inductors and interdigitated capacitors. The following chapter outlines the results and conclusions from our designs and methodologies.

4.1 SPIRAL INDUCTOR

To model spiral inductors, we used ANSYS Designer® which proved to be very effective for simulating two dimensional inductors. Geometries with hexagonal, octagonal, circular, and square coils were all considered [6]. Micro-dispensing is best when printing continuous lines instead of lines with sharp corners. Discontinuities in the motion of the print head can cause material accumulation at these points. Therefore, circular inductors were chosen because the circular spirals can be printed with a continuous process. The outer diameter of the inductor is just over 2.0 mm providing a value of 150 nH. Figure 4.1 shows the model design versus the printed results for the inductor. Table 4.1 compares the modeled parameters to the measured values obtained in the lab. Finally, Fig. 4.2 compares the modeled results to the experimental results over a frequency range between 0.1 MHz and 2 MHz.

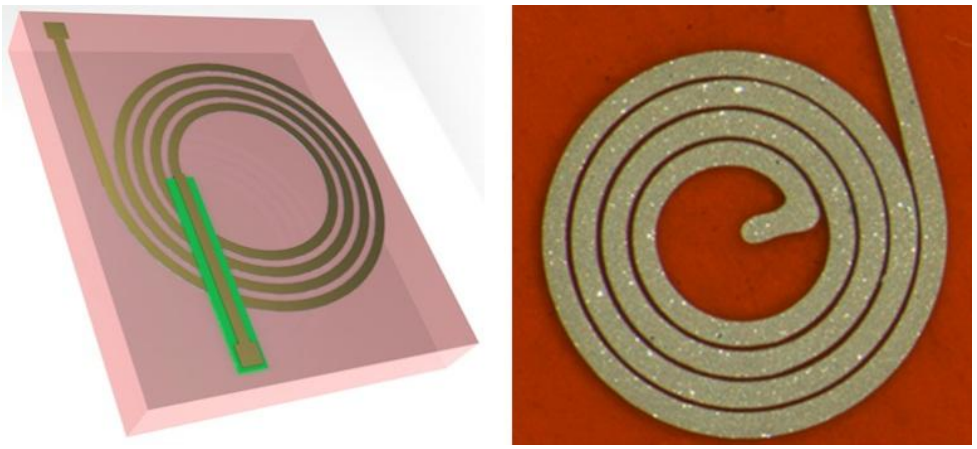

Figure 4.1 (Left) Modeled spiral inductor. (Right) Printed spiral inductor.

TABLE 4.1: Values for Printed Spiral Inductors

Parameter	***Modeled***	***Measured***	***Units***
# turns	4	4	turns
Spacing between spirals	110	110.8	μm
Trace width	170	170.6	μm
Minimum L	150	158.2	nH
Maximum L	150	168.5	nH

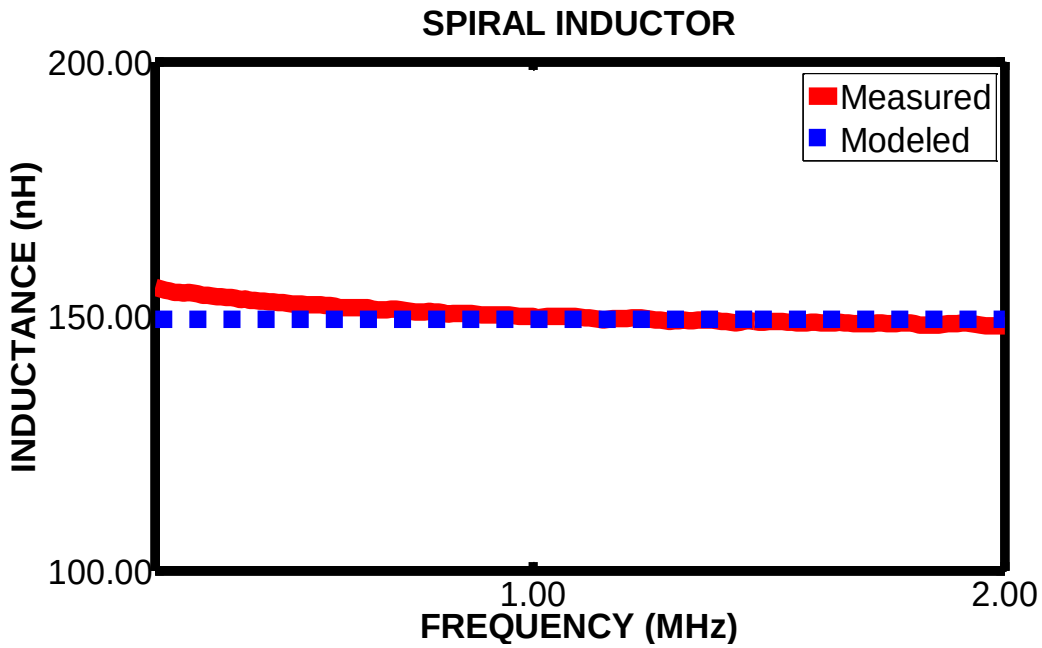

Figure 4.2: Frequency sweep comparing model to measured results for spiral inductor.

4.2 INTERDIGITATED CAPACITOR

We also used ANSYS Designer® to design an interdigitated capacitor to be 12 pF [7]. The outer dimension of the capacitor was just over 5.0 mm. Table 4.2 compares the modeled parameters to the measured. Furthermore, Figure 4.3 shows the model results versus the measured results from the constructed device. Figure 4.4 compares the modeled results to the experimental results over a frequency range from 0.1 MHz to 2 MHz.

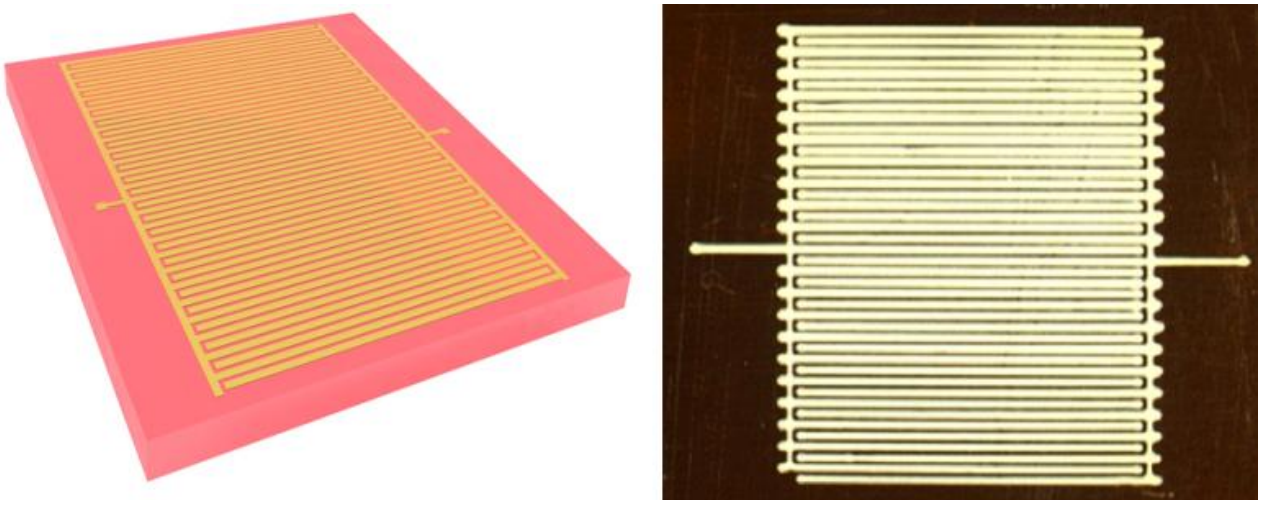

Figure 4.3: (Left) Modeled interdigitated capacitor. (Right) Printed interdigitated capacitor.

TABLE 4.2: Values for Printed Interdigitated Capacitors

Parameter	***Modeled***	***Measured***	***Units***
# fingers	4	4	fingers
Spacing between fingers	60	60.34	μm
Trace width	140	156.3	μm
Minimum C	12	10.34	pF
Maximum C	12	12.42	pF

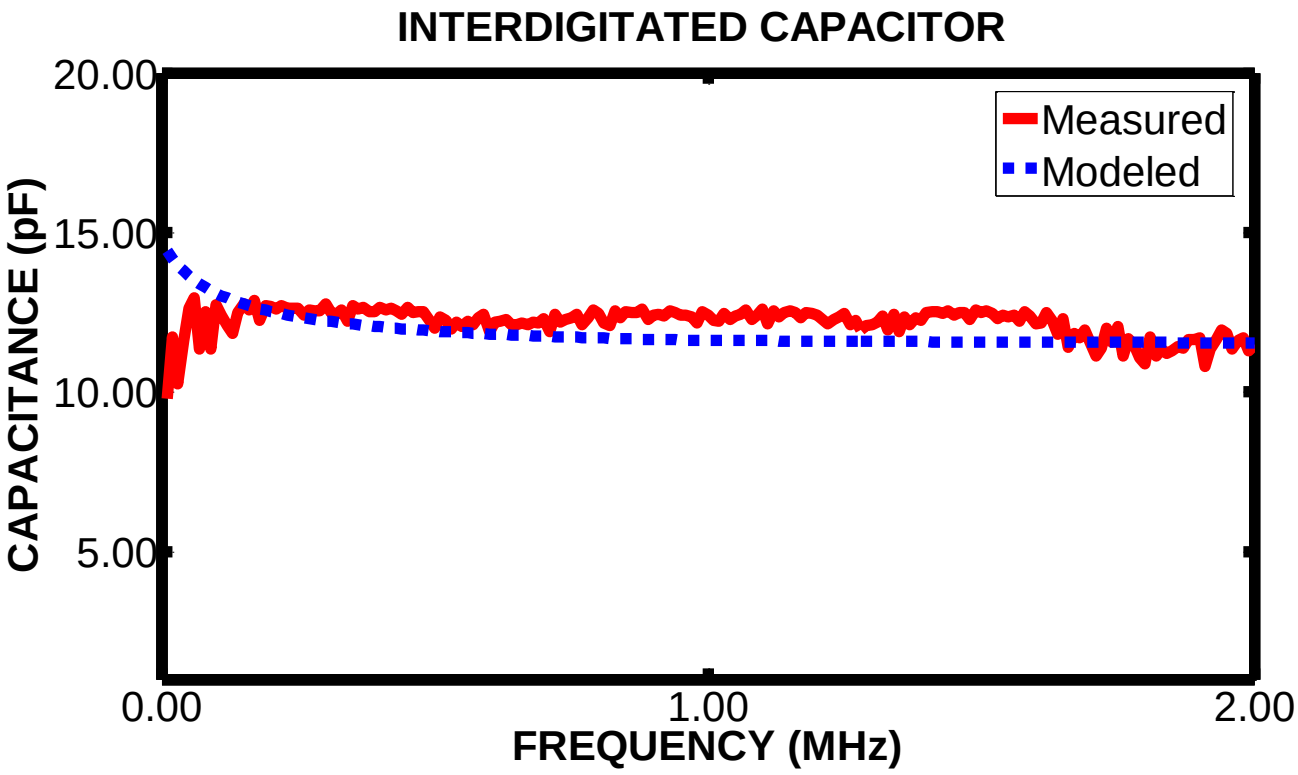

Figure 4.4: Frequency sweep comparing model to measured results for interdigitated capacitor.

CHAPTER 5
SUMMARY AND CONCLUSIONS

3D printing has evolved over the last ten years from a rapid prototyping tool to a true manufacturing technology capable of producing functional products. In order to manufacture the products of tomorrow by 3D printing, it is necessary to print electrical components. In this work, we designed planar inductors and capacitors and manufactured them by micro-dispensing. This 3D printing technique was chosen because it currently offers the greatest potential to print circuits in 3D printed devices. The impedance elements were measured and results compared very well to the measured results. Capacitors were printed within 20% of their design value and inductors were printed within 10%. Future work will entail improving device tolerances, printing elements with high impedance, building functional circuit, incorporating impedance elements into antennas or frequency selective surfaces, and perhaps printing active devices.

REFERENCES

[1] Gibson, Ian, David W. Rosen, and Brent Stucker. Additive manufacturing technologies: rapid prototyping to direct digital manufacturing. Springer, 2010.

[2] R. D Mancosu, J.A.Q Quintero, R. E S Azevedo, "Sintering, in different temperatures, of traces of silver printed in flexible surfaces," Thermal, Mechanical & Multi-Physics Simulation, and Experiments in Microelectronics and Microsystems (EuroSimE), 2010 11th International Conference on , vol., no., pp.1,5, 26-28 April. 2010 Nokia Inst. of Technol. INdT, Manaus, Brazil.

[3] K. Nam-Soo, H. N. Kenneth (2010, Nov.). "Future Direction of Direct Writing," J. Appl. Phys. 108, 102801[Online]. Availiable: http://dx.doi.org/10.1063/1.3510359

[4] K. Church, E. MacDonald, P. Clark, R. Taylor, D. Paul, K. Stone, M. Wilhelm, F. Medina, J. Lyke, R. Wicker, "Printed electronic processes for flexible hybrid circuits and antennas," Flexible Electronics & Displays Conference and Exhibition, 2009. , vol., no., pp.1,7, 2-5 Feb. 2009.

[5] Li, P.A. Clarck, and K.H. Church, "Robust Direct-Write Dispense Tool and Solutions for Micro/Meso-Scale," Proceedings of the 2007 International Manufacturing Science And Engineering Conference,MSEC2007.October 15-17, 2007, Atlanta, Georgia, USA.

[6] S. S. Mohan, M. M. Hershenson, S. P. Boyd, and T. H. Lee, "Simple Accurate Expressions for Planar Spiral Inductances," *IEEE Journal of Solid-State Circuits*, Vol. 34, No. 10, pp. 1419–1424, 1999.

[7] G. D. Alley, "Interdigital Capacitors and Their Application to Lumped-Element Microwave Integrated Circuits," *IEEE Trans. Microwave Theory and Techniques*, Vol. MTT-18, No. 12, pp. 1028–1033, 1970.

[8] Jiing-Liang Wu; E.S. Ortoli, D.T. Hackworth, "Electrical Insulation Performance Comparisons between Kapton and Teflon Coil Insulation Systems for Pulse Power Applications," Electromagnetic Launch Technology, 2008 14th Symposium on , vol., no., pp.1,6, 10-13 June 2008.

CURRICULUM VITA

Ubaldo Robles Dominguez was born in Cd. Juarez, Chihuahua, Mexico. The third son of Eduardo Robles Sandoval and Dalia Dominguez Carrasco, he graduated from El Chamizal High School, Cd. Juarez, Chihuahua, Mexico. In fall 2000, Ubaldo entered The University of Texas at El Paso as an International Student. While pursuing a bachelor's degree in electrical engineering, he worked as a peer leader and tutor in the University of Texas at El Paso, during the years 2002-2006 he cofounded and managed the SOLAPSUS café and tutoring center for students in Cd. Juarez, Mexico, while staying a student and a tutor in college. Later on, Ubaldo became the founder of the Automated Engineering Association in El Paso, TX. As an Electrical Engineer he worked as a Circuit Designer in the University of Texas at El Paso under several projects. Finally, in 2008 Ubaldo took the responsibility of managing the measurements laboratory for the Electromagnetics Laboratory in the W.M. Keck Center for 3D Innovation while pursuing his Master's Degree in Science for Electrical Engineering. Ubaldo Robles has won "Best Student Presentation Award." And "Outstanding Paper Award" during IMAPS Advanced Technology Workshop on RF and Microwave Packaging. San Diego CA. February 7-8, 2012. Currently, Ubaldo Robles is pursuing his Doctoral Degree in Electrical Engineering while maintaining a research position and managing the measurements laboratory in the W.M. Keck Center for 3D innovation.

Permanent Address: 5624 Joyce Cir.
El Paso, Texas 79904
Or
Ubaldo.Robles@gmail.com